Desalination and Water Treatment
www.deswater.com

doi:10.5004/dwt.2016.0055

61 (2017) 50–57
January

Analysis of combined influence of foulant concentration and flux in ultrafiltration membrane process using response surface methodology

Yongsun Jang[a], Yongjun Choi[a], Younghoon Ko, Sangho Lee[a,*], Jaewuk Koo[a, b], Youn-Jong Park[c]

[a]*School of Civil and Environmental Engineering, Kookmin University, Jeongneung-Dong, Seongbuk-Gu, Seoul, 136-702, Republic of Korea, email: cutymonkey5@naver.com (Y. Jang), email: choiyj1041@gmail.com (Y. Choi), email: rhddudgnd@naver.com (Y. ko), Tel. 8229104529, Fax 8229104939, email: sanghlee@kookmin.ac.kr (S. Lee)*
[b]*Korea Institute of Construction Technology, 2311 Daehwa-Dong, Ilsan-Gu, Goyang-Si, Gyeonggi-Do, 411-712, South Korea, email: koojaewuk@kict.re.kr*
[c]*SK Engineering and Construction, 192-18 Gwanhoon-dong, Jongno-gu, Seoul, Korea, email: yjpark07@sk.com*

Received 14 January 2016; Accepted 23 August 2016

ABSTRACT

Microfiltration (MF) and ultrafiltration (UF) have been extensively adopted as alternatives to conventional filtration. However, one of the main barriers to widespread use of these technologies is membrane fouling that affects both the quality and the quantity of the product water. Accordingly, the operation conditions for MF/UF should be properly adjusted to minimize fouling. The objective of this study is to analyze combined influence of foulant concentration and flux on fouling propensity of hollow fiber UF membrane through response surface methodology and Central Composite Design. Colloidal silica, kaolin and alginate were used as model foulants, and the concentration of foulant and flux were chosen as the operation parameter. In each case, the fouling rate was determined based on the experimental results. Second-order polynomial model equations were derived to predict the fouling rate as a function of foulant concentration and flux. Finally, operating conditions for a given level of fouling were determined using the model equation and the optimization plot.

Keywords: Microfiltration (MF); Ultrafiltration (UF); Fouling; Flux; Response surface methodology (RSM)

1. Introduction

One of the most pervasive problems afflicting people in the world is inadequate access to clean water and sanitation. Due to an increase in population and water demand, water scarcity is expected to grow worse in the coming decades. Addressing these problems calls out for a tremendous amount of research to be conducted to identify robust new methods of purifying water at lower cost, minimizing impact on the environment. Membrane-based water treatment technology is considered as a highly competitive and promising candidate for developing water sources to meet this challenge [1–6].

Microfiltration (MF) and ultrafiltration (UF) are being widely applied to remove turbidity, microorganisms and natural organic matter (NOM) in drinking water and wastewater. They can also serve as a pretreatment for more advanced processes such as reverse osmosis (RO) [7–12]. Especially, MF and UF membrane applications are receiving increased attention associated with water quality and cost reduction by improvements in membrane technology [13,14].

However, one of the main barriers to greater use of the membrane technologies is membrane fouling, which is

*Corresponding author.

Presented at the 8th International Conference on Challenges in Environmental Science & Engineering (CESE-2015), 28 September–2 October 2015, Sydney, Australia.

1944-3994 / 1944-3986 © 2017 Desalination Publications. All rights reserved.

caused by deposition and/or adsorption of water impurities such as organic substances and particulates, on the membrane surface and/or pores. As a result, the productivity of the membranes declines significantly with filtration time. Membrane fouling affects both the quality and the quantity of the product water [15–18]. Membrane performance could be recovered through cleaning process which increases the energy consumption and operational complexity. As a result, a lot of studies have been carried out toward better understanding and control of membrane fouling [19–23].

The objective of this study is to analyze the combined influence of foulant concentration and flux for hollow fiber UF membrane process through response surface methodology (RSM). RSM is an effective statistical tool to solve multi-variable problems, analyze the interactions among factors, and optimize one or several responses in which multiple variables may influence the outputs based on the Central Composite Design (CCD). RSM is especially useful to reduce the number of experimental trials needed to evaluate multiple parameters and their interactions [23–27]. Accordingly, there are many previous studies to optimize UF membrane operation conditions using RSM in water treatment or fruit juice manufacturing [25,28]. In this study, hydrophobic hollow fiber UF membranes were used, and synthetic feed waters containing different types of foulants were used. Kaolin was used to simulate particulate foulant in natural water, and colloidal silica was selected to represent colloidal foulants. Alginate was used to reflect the effect of polysaccharide-based organic matters caused by algae, which is one of the problems in surface water treatment. In fact, these have been widely adopted for previous MF/UF experiments [29,30]. The concentration of foulant and permeate flux were selected as key operation parameters. In fact, temperature is another important factor affecting the fouling behaviors of UF membranes. However, this study mainly focused on the combined effect of flux and foulant concentration under constant temperature conditions. Using fouling rates obtained from different experiment conditions, the RSM analysis was carried out.

2. Materials and methods

2.1. Laboratory-scale submerged membrane system

A schematic diagram of laboratory-scale submerged hollow fiber membrane system is shown in Fig. 1. The system consists of membrane modules, feed tanks, digital pressure sensors, a multi-channel pump, a stirrer and a computer for data logging. The volume of each feed tank was 1 L. A single hollow fiber membrane was submerged in each feed tank and connected with suction hose. Permeate water from the hollow fiber membrane is recirculated by a multi-channel pump (EW-07551-00, Cole-Parmer, USA). When permeation pass through digital pressure gauge (ISE40A-01-R, SMC, JAPAN), transmembrane pressure (TMP) was recorded in every seconds and stored in the desktop. Flow type was outside-in mode, and the temperature of feed water was kept at 20°C. The pump was operated to maintain a constant permeate flux through the experiments. Up to 15 simultaneous filtration experiments could be carried out using this experimental setup.

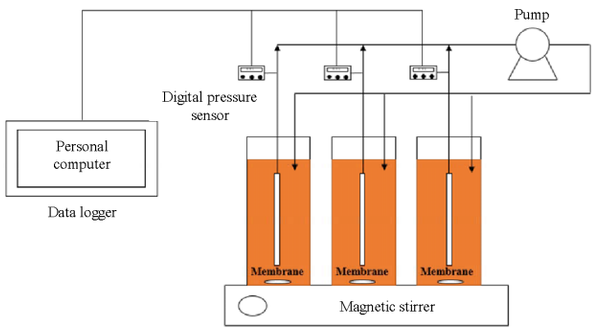

Fig. 1. Experimental setup for submerged UF test.

2.2. UF membranes

Hydrophobic PVDF hollow fiber membranes manufactured by Samsung SDI were used. Prior to experiments, membranes were wetted using methanol and water. Because pump was operated in the constant flux mode, flux was varied by changing length of membranes. The length of membrane corresponded to flux is summarized in Table 1. The length of membrane was given a variety from 36 to 180 mm according to flux. They have a nominal pore size of 4.87±0.87 nm and a nominal diameter of 2.1 mm as shown in Table 2.

2.3. Preparation of feed solutions

Model foulants used in this study were commercially available alginate (alginic acid sodium salt from brown algae, Sigma-Aldrich), LUDOX TMA colloidal silica (Sigma-Aldrich)

Table 1
The length of the membrane fiber and the corresponding flux

Length of membrane (mm)	Flux (L m^{-2}-h^{-1})
36	250
72	200
108	150
144	100
180	50

Table 2
Specifications of the hollow fiber UF membrane

Membranes specifications	
Filtration method	Dead-end
Properties	Hydrophobic
Material	PVDF
Nominal pore size	4.87 ± 0.87 nm
Nominal diameter	2.1 mm
Length	36–180 mm

and kaolin (Sigma-Aldrich, K7375). Particle sizes of colloidal silica according to manufacturer was 22 nm, and the molecular weight of alginate was $3.50\pm0.04\times10^5$ g mol^{-1}. Also, the range of particle sizes of kaolin was from 0.1 to 4 μm [31–33]. Feed waters were prepared by mixing the model foulants with deionized (DI) water.

2.4. Calculation of fouling rates

The fouling rate, which is defined as the rate of TMP increase, was selected as a quantitative index to indicate membrane fouling. This is based on a simple filtration model for a dead-end MF/UF system. Details on the determination of the fouling rate have been reported in our previous publication [34].

Prior to fouling tests, all membranes were filtered by DI water to obtain net TMP which can be measured by calculating the difference of TMP with feed water and DI water. In all experiments, operating time was 3 h both DI water and fouling tests. After net TMP values were obtained for each foulant, net TMP curve for operating time was drawn, and the slope of the linear region was calculated as the fouling rate.

2.5. Design of experiment

In the RSM analysis, two variable (foulants concentration and permeate flux) and five level (-1.41, -1, 0, 1, 1.41) conditions were used for each foulant (kaolin, alginate, silica), and the fouling rate was the response (Y). CCD was performed using a statistical analysis software (Minitab® 16.2.0, Minitab, USA). The experimental design is shown in Table 3.

2.6. Regression analysis

To predict the dependence of fouling rate on flux and foulant concentration, regression analysis was performed.

Table 3
Variables design for RSM analyzing

Run order	X_1 (Concentration)	X_2 (Flux)
1	0 (30 mg L^{-1})	0 (150 LMH)
2	0 (30 mg L^{-1})	1.41 (250 LMH)
3	0 (30 mg L^{-1})	0 (150 LMH)
4	1 (40 mg L^{-1})	–1 (100 LMH)
5	0 (30 mg L^{-1})	0 (150 LMH)
6	–1 (20 mg L^{-1})	1 (200 LMH)
7	0 (30 mg L^{-1})	0 (150 LMH)
8	1.41 (50 mg L^{-1})	0 (150 LMH)
9	–1.41 (10 mg L^{-1})	0 (150 LMH)
10	0 (30 mg L^{-1})	0 (150 LMH)
11	0 (30 mg L^{-1})	–1.41 (50 LMH)
12	–1 (20 mg L^{-1})	–1 (100 LMH)
13	1 (40 mg L^{-1})	1 (200 LMH)

Using the results in the fouling experiments, a set of second-order polynomial equation was derived:

$$Y_k = \beta_{k0} + \sum_{i=1}^{4}\beta_{ki}X_i + \sum_{i=1}^{3}\sum_{j=i+1}^{4}\beta_{kij}X_iX_j + \sum_{i=1}^{4}\beta_{kii}X_i^2 \quad (1)$$

where Y_k are the response (fouling rate); β_{k0}, β_{ki}, β_{kii} and β_{kij} are the regression coefficients; and X_i and X_j are the coded independent variables (flux and foulant concentration, respectively). The correlation coefficient (R^2) was evaluated for the examination of the accuracy of the model [27].

3. Results and discussion

3.1. Comparison of fouling rates for different foulants

A series of experiments for each foulant were carried out based on the design of experiment in Table 3. The foulant concentration ranged from 10 to 50 mg L^{-1}, and the flux ranged from 50 to 250 L m^{-2}-h^{-1}. TMP was measured for each case, and the fouling rate was calculated from the slope of TMP profile. The fouling rate was selected as the response for the RSM analysis. The results are shown in Fig. 2.

In the case of alginate, the fouling rate was relatively high compared with the other two foulants as shown in Fig. 2(a). This is attributed to the higher affinity of alginate to membrane surfaces than colloidal silica and kaolin. Moreover, shear force near the membrane surface is not effective to prevent foulant layer formation by alginate because it is a dissolved material. Accordingly, alginate can easily form gel layer on the membrane surface after its adsorption, leading to reduced permeability. Similar results can be also found in previous studies [35,36]. The fouling rate ranges from 0 to 0.0013 bar min^{-1}, and its variations are significant. The maximum fouling rate was observed when the alginate concentration and the flux were 50 mg L^{-1} and 150 L m^{-2}-h^{-1}, respectively. Negligible fouling rates were obtained in the run order 2, 6, 11 and 12. It appears the effect of flux and concentration on fouling rate is complicated due to the combined influences. As shown in Fig. 2(b), the fouling rates of colloidal silica were generally lower than those of alginate. Under similar conditions, although the maximum fouling rate was presented in the case of silica as shown in Fig. 2(b), run order 8, it is likely that alginate results in higher fouling propensity than silica. On the other hand, the fouling rates of kaolin were much lower than those of alginate and silica. It is evident from the results that kaolin has lower fouling potential than alginate and silica. Based on the results, it is likely that the affinity of silica and kaolin to membrane surfaces is lower than that of alginate. Moreover, the difference in fouling rates between silica and kaolin may be attributed to the particle size differences. Since the silica has particle size that is similar to the membrane pore size, pore blocking may occur, leading to substantial fouling. On the other hand, kaolin has particle size larger than the pore size and thus has limited fouling potential [37,38].

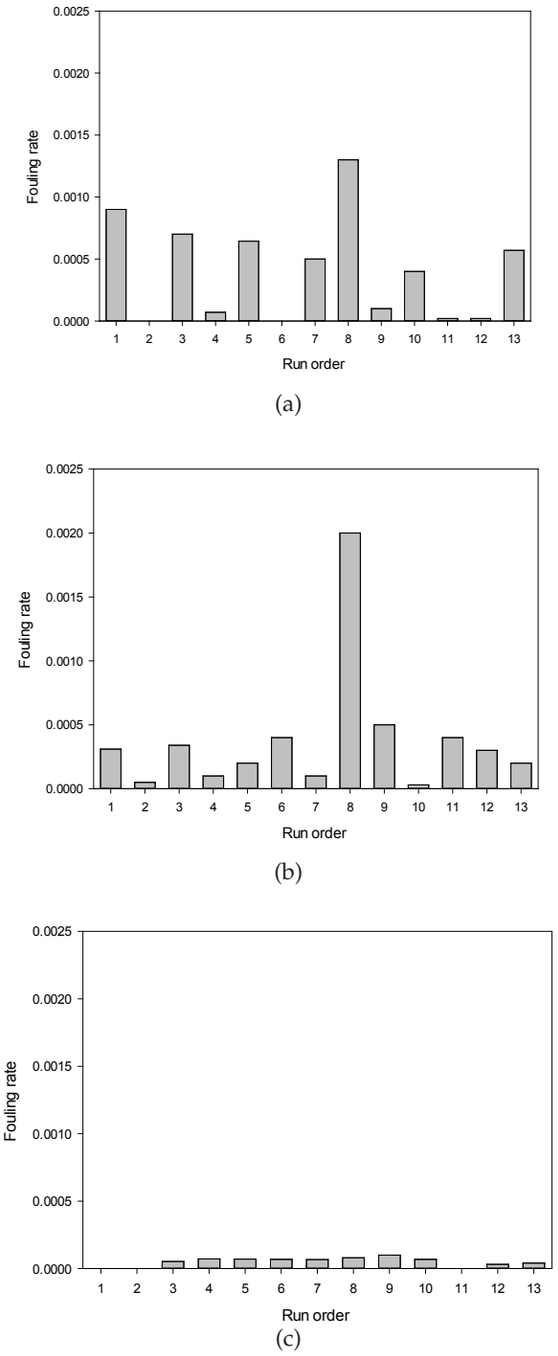

Fig. 2. The responses (fouling rates) of (a) alginate, (b) silica and (c) kaolin from fouling experiments.

3.2. RSM analysis

Since the relationship between fouling rate and operation conditions (flux and foulant concentration) is not simple, it is necessary to apply a statistical method to analyze it. As mentioned earlier, the RSM was used to derive models to predict fouling rate as a function of flux and foulant concentration. Based on the results in Fig. 2, second-order polynomial models were obtained using the statistical analysis software:

$$Y_{alginate} = 4.90 \times 10^{-4} - 2.11 \times 10^{-5}X_1 + 1.22 \times 10^{-5}X_2 + 1.22 \times 10^{-7}X_1^2 - 6.41 \times 10^{-8}X_2^2 + 2.6 \times 10^{-7}X_1X_2 \quad (2)$$

$$Y_{silica} = 7.19 \times 10^{-4} - 8.57 \times 10^{-4}X_1 + 6.43 \times 10^{-6}X_2 + 2.62 \times 10^{-6}X_1^2 + 2.43 \times 10^{-9}X_2^2 - 3 \times 10^{-7}X_1X_2 \quad (3)$$

$$Y_{kaolin} = -1.23 \times 10^{-4} - 9.41 \times 10^{-7}X_1 + 2.57 \times 10^{-6}X_2 + 9.71 \times 10^{-8}X_1^2 - 5.11 \times 10^{-9}X_2^2 - 3.41 \times 10^{-8}X_1X_2 \quad (4)$$

where $Y_{alginate}$, Y_{silica} and Y_{kaolin} are the fouling rates of alginate, silica and kaolin, respectively. X_1 is the flux, and the X_2 is the foulant concentration. The confidence level of these models was 95%. The R^2 values were larger than 70%, which implies that these equations were useful to predict fouling rates. Considering the facts that there are a lot of factors affecting the results of fouling experiments, the results seem to be acceptable.

3.3. Combined effect of flux and foulant concentration on fouling rate

The reliability of the model equations was verified according to the analysis of variance (ANOVA) method [25–28]. The results of ANOVA for the model equations are summarized in Table 4. The F-values of the regression models for alginate, silica and kaolin were 3.93, 3.70 and 3.52, respectively, and their p-values were less than 0.66, which suggests that the models are statistically significant. Moreover, the p-values for the lack-of-fit were larger than 0.059, indicating that these models properly describe the functional relationship between the experimental factors and the response variable.

The effects of flux and foulant concentration and their interaction on fouling rate are illustrated as response surfaces and contour plots in Figs. 3, 4 and 5. The RSM Eqs. (2), –(4) were used to create these plots for alginate, silica and kaolin, respectively. The response surfaces show the overall trends of the fouling rate as a function of flux and foulant concentration while the contour plots present the values for fouling rate for given conditions.

The plots in Fig. 3 show the response surface and contour plot for the fouling rate by the alginate. As shown in Fig. 3(a), the fouling rate does not linearly depend on flux and foulant concentration. As flux increases, the fouling rate increases at high foulant concentrations. However, it increases and decreases at low foulant concentrations. The fouling rate increases with increasing foulant concentration at high flux conditions, but it does not depend on foulant concentration at low flux conditions. As shown in Fig. 3(b), the maximum fouling rate is expected to be obtained at 200 L m^{-2}-h^{-1} and 50 mg L^{-1}. These results suggest that the fouling by alginate results from complex interactions between flux and foulant concentration.

The plots in Fig. 4 show the response surface and contour plots for silica fouling. The results are quite different

Table 4
Analysis of variance of the experimental results

Model foulant	Source	Degree of freedom	F-value	p-value
Alginate	Regression	5	3.93	0.050
	Linear	2	1.88	0.222
	Concentration	1	0.15	0.712
	Flux	1	1.23	0.304
	Square	2	4.35	0.059
	Concentration	1	0.04	0.840
	Flux	1	7.63	0.027
	Interaction	1	0.88	0.381
	Concentration × flux	1	0.88	0.381
	Lack-of-fit	3	3.54	0.127
Silica	Regression	5	3.70	0.059
	Linear	2	3.39	0.093
	Concentration	1	3.79	0.093
	Flux	1	0.01	0.930
	Square	2	6.86	0.022
	Concentration	1	12.70	0.009
	Flux	1	0.0	0.0963
	Interaction	1	0.0	1.000
	Concentration × flux	1	0.0	1.000
	Lack-of-fit	3	14.78	0.012
Kaolin	Regression	5	3.52	0.066
	Linear	2	8.33	0.014
	Concentration	1	0.04	0.843
	Flux	1	7.88	0.026
	Square	2	7.65	0.017
	Concentration	1	4.04	0.084
	Flux	1	7.01	0.033
	Interaction	1	2.17	0.184
	Concentration × flux	1	2.17	0.184
	Lack-of-fit	3	0.09	0.960

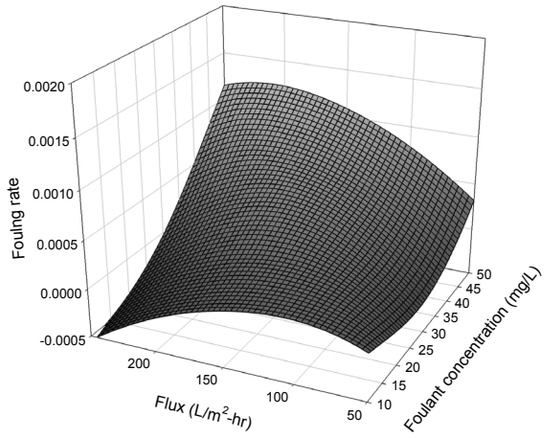

(a)

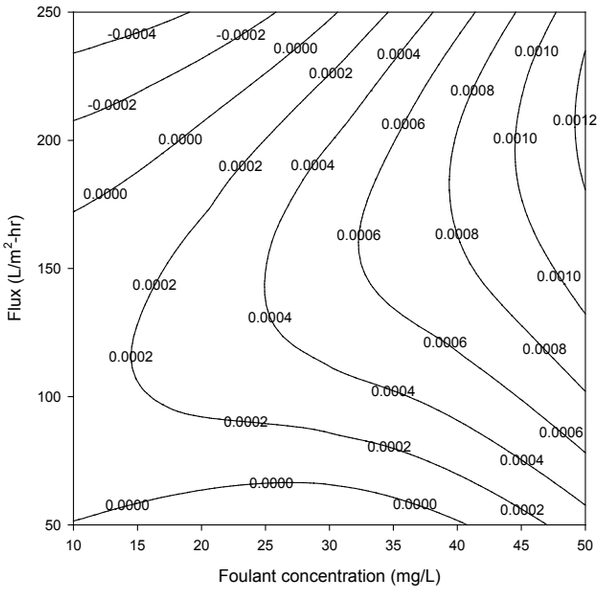

(b)

Fig. 3. Dependence of fouling rate on flux and alginate concentration: (a) response surface and (b) contour plot.

from those for alginate fouling. As shown in Fig. 4(a), the flux does not affect the fouling rate when the foulant concentration is low. However, the effect of flux becomes more important as the foulant concentration increases. Moreover, the fouling rate showed minimum values at the foulant concentration of 25 mg L^{-1}. This might be attributed to the aggregation of silica during the membrane filtration. At low concentration, silica colloids exist individually in the solution or near the membrane surface. As the concentration increases, silica colloids may form aggregates, and the fouling potential may decrease. Above a critical concentration, however, the silica aggregates can also cause rapid membrane fouling due to their high concentrations. Fig. 4(b) also clearly shows the changes in fouling rate by flux and silica concentration. The fouling rates range from 0 to 0.0020 bar min^{-1}.

The final case is the fouling by kaolin as shown in Fig. 5. Unlike the other cases, the fouling rates were relatively low for all flux and foulant concentration conditions as shown in Fig. 5(a). Accordingly, the shape of the contour plot in Fig. 5(b) is not meaningful. It is evident that the fouling by kaolin is not serious compared with those by alginate and silica. Similar results are also reported by the other study [27]. The fouling rate changes with flux and foulant concentration but the dependence does not seem to be important.

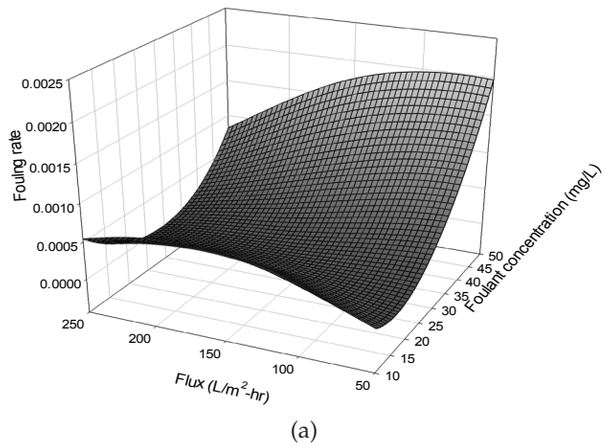

(a)

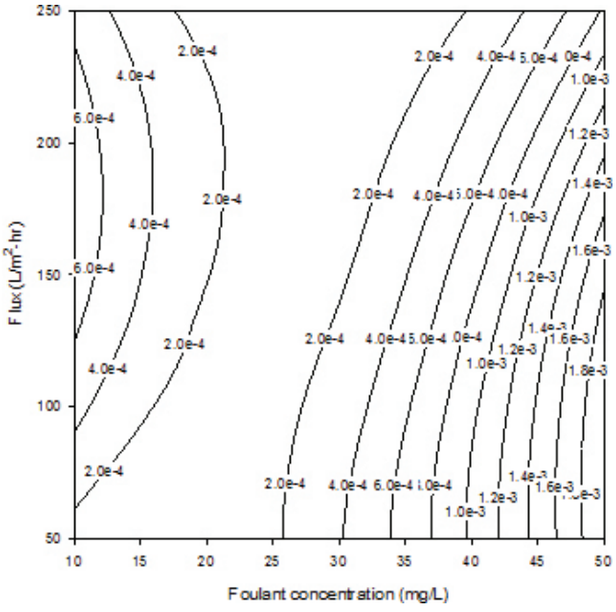

(b)

Fig. 4. Dependence of fouling rate on flux and silica concentration: (a) response surface and (b) contour plot.

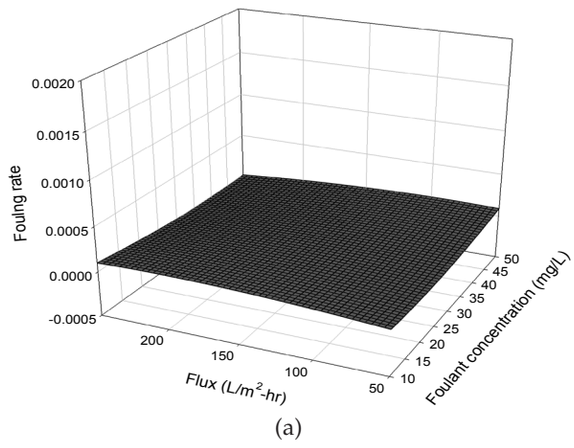

(a)

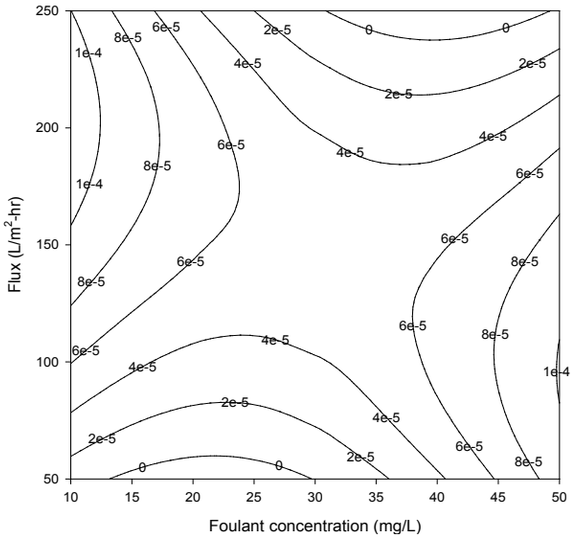

(b)

Fig. 5. Dependence of fouling rate on flux and kaolin concentration: (a) response surface and (b) contour plot.

3.4. Determination of the operating condition for a given fouling rate

The RSM Eqs. (3)–(5) indicate that there are a couple of conditions to result in a specific fouling rate. Among these conditions, the condition for best match to the given (or target) fouling rate exists. Of course, this condition may change using a different value of the fouling rate. Nevertheless, it is meaningful to determine the best match (or "optimum") conditions for flux and foulant concentration that lead to the target fouling rate.

Fig. 6 shows the optimization plots for alginate and silica with the target fouling rate of 0.0005 bar min^{-1}. The results using kaolin were not used for this analysis because the fouling rate was always lower than 0.0005 bar min^{-1} for all conditions. The composite desirability evaluates how the conditions optimize the fouling rate. The desirability has a range of zero to one, and one represents the ideal case. As shown in Fig. 6(a), the best match of the target fouling rate for alginate was found at 250 L m^{-2}-h^{-1} and 40 mg L^{-1}. Similarly, the best match of the target fouling rate for silica was found at 250 L m^{-2}-h^{-1} and 44 mg L^{-1} as shown in Fig. 6(b).

If the target of the fouling rate changes, the best match conditions may be changed. Fig. 7 shows the optimization plots for alginate and silica with the target fouling rate of 0.001 bar min^{-1}. The best match conditions of the target fouling rate for alginate were 136 L m^{-2}-h^{-1} and 50 mg L^{-1} while those for silica were 50 L m^{-2}-h^{-1} and 38 mg L^{-1}.

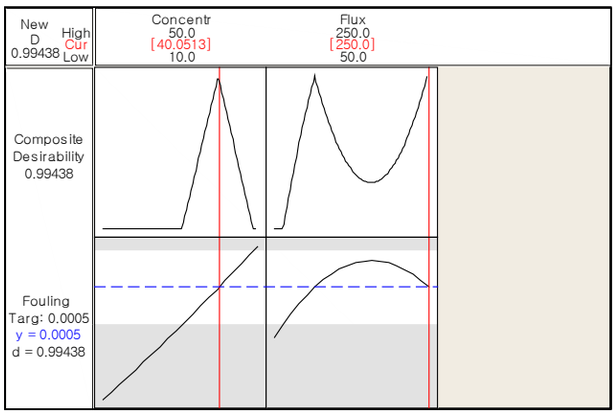

(a)

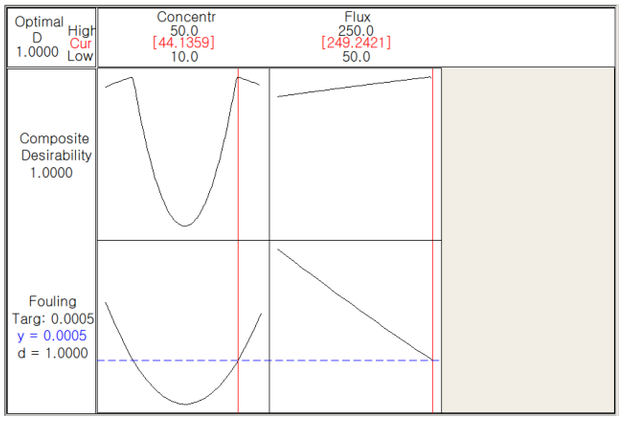

(b)

Fig. 6. Optimization plot at the target fouling rate of 0.0005 bar min^{-1}: (a) alginate and (b) silica.

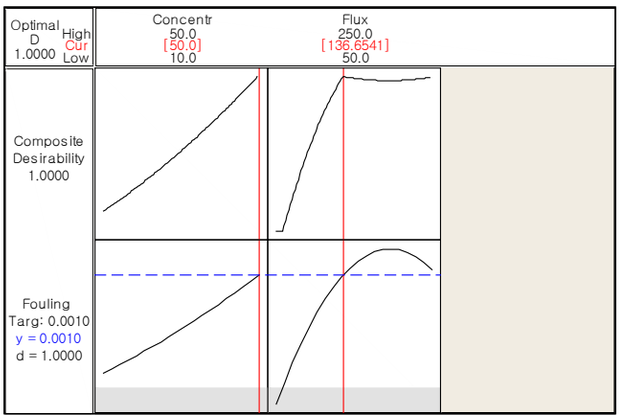

(a)

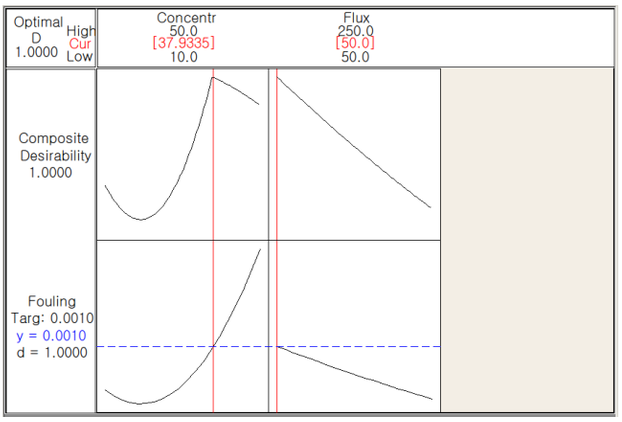

(b)

Fig. 7. Optimization plot at the target fouling rate of 0.001 bar min^{-1}: (a) alginate and (b) silica.

4. Conclusions

In this study, the combined effects of foulant concentration and flux on fouling propensity of hollow fiber UF membrane were quantitatively analyzed by applying RSM and CCD. The following conclusions were withdrawn:

(1) The fouling rates for alginate, silica and kaolin were determined to quantify fouling propensity. The fouling rate of alginate was higher than those of silica and kaolin under similar flux and concentration. Kaolin only showed insignificant fouling potential under the test conditions. The dependence of fouling rate on flux and concentration was complex for all cases.

(2) Using RSM, second-order polynomial models were established by regression analysis to predict effect of flux and foulant concentration on fouling rate in a laboratory-scale UF system.

(3) The surface and contour plots from the RSM analysis also show the complicated relationships between fouling rate and operation parameters (flux and foulant concentration). An optimization plot was obtained for each foulant to find out the best match conditions of flux and foulant concentration for a given fouling rate.

Acknowledgment

This research was supported by Korea Ministry of Environment as "The Eco-Innovation project (Global Top project)" (GT-SWS-11-02-007-9).

References

[1] M.A. Shannon, Science and technology for water purification in the coming decades, Nature, 452 (2008) 301–310.

[2] J.Xu, Constructing antimicrobial membrane surfaces with polycation-copper (II) complex assembly for efficient seawater softening treatment, J. Membr. Sci., 491 (2015) 28–36.

[3] W.L. Ang, A review on the applicability of integrated/hybrid membrane processes in water treatment and desalination plants, Desalination, 363 (2015) 2–18.

[4] X. Qu, Applications of nanotechnology in water and wastewater treatment, Water Res., 47 (2013) 3931–3946.

[5] R. Lopez-Roldan, Assessment of the water chemical quality improvement based on human health risk indexes: application to a drinking water treatment plant incorporating membrane technologies, Sci. Total Environ., 540 (2016) 334–343.

[6] J. Yin, Polymer-matrix nanocomposite membranes for water treatment, J. Membr. Sci., 479 (2015) 256–275.

[7] B. Malczewska, Virtual elimination of MF and UF fouling by adsorptive pre-coat filtration, J. Membr. Sci., 479 (2015) 159–164.
[8] L. Fiksdal, The effect of coagulation with MF/UF membrane filtration for the removal of virus in drinking water, J. Membr. Sci., 279 (2006) 364–371.
[9] K.J. Howe, Effect of membrane configuration on bench-scale MF and UF fouling experiments, Water Res., 41 (2007) 3842–3849.
[10] A.R. Guastalli, Comparison of DMF and UF pre-treatments for particulate material and dissolved organic matter removal in SWRO desalination, Desalination, 322 (2013) 144–150.
[11] Y. Xiao, Feasibility of using innovative PVDF MF membrane prior to RO for reuse of a secondary municipal effluent, Desalination, 311 (2013) 16–23.
[12] L.O. Villacorte, MF/UF rejection and fouling potential of algal organic matter from bloom-forming marine and freshwater algae, Desalination, 367 (2015) 1–10.
[13] N. Lee, Identification and understanding of fouling in low-pressure membrane (MF/UF) filtration by natural organic matter (NOM), Water Res., 38 (2004) 4511–4523.
[14] G.K. Pearce, UF/MF pre-treatment to RO in seawater and wastewater reuse applications: a comparison of energy costs, Desalination, 222 (2008) 66–73.
[15] D. Chen, Enzymatic control of alginate fouling of dead-end MF and UF ceramic membranes, J. Membr. Sci., 381 (2011) 118–125.
[16] G. Zin, Fouling control in ultrafiltration of bovine serum albumin and milk by the use of permanent magnetic field, Journal of Food Engineering, 168 (2016) 154–159.
[17] J. Tian, $KMnO_4$ pre-oxidation combined with $FeCl_3$ coagulation for UF membrane fouling control, Desalination, 320 (2013) 40–48.
[18] Y.-J. Won, Correlation of membrane fouling with topography of patterned membranes for water treatment, J. Membr. Sci., 498 (2016) 14–19.
[19] J. Tian, Effect of different cations on UF membrane fouling by NOM fractions, Chemical Engineering Journal, 223 (2013) 547–555.
[20] S. Walker, Hollow fiber ultrafiltration of Ottawa River water: floatation versus sedimentation pre-treatment, Chem. Eng. J., 288 (2016) 228–237.
[21] J. Tian, Correlations of relevant membrane foulants with UF membrane fouling in different waters, Water Res, 47 (2013) 1218–1228.
[22] M.F. Rabuni, Impact of in situ physical and chemical cleaning on PVDF membrane properties and performances, Chem. Eng. J., 122 (2015) 426–435.
[23] C. Regula, Chemical cleaning/disinfection and ageing of organic UF membranes: a review, Water Res, 56 (2014) 325–365.
[24] N. Javadi, Experimental studies and statistical analysis of membrane fouling behavior and performance in microfiltration of microalgae by a gas sparging assisted process, Bioresour. Technol., 162 (2014) 350–357.
[25] R.A.R. Figueroa, Ultrafiltration of orange press liquor: optimization for permeate flux and fouling index by response surface methodology, Sep. Purif. Technol., 80 (2011) 1–10.
[26] H. Fu, Effects of aeration parameters on effluent quality and membrane fouling in a submerged membrane bioreactor using Box–Behnken response surface methodology, Desalination, 302 (2012) 33–42.
[27] Y. Kim, Modeling fouling of hollow fiber membrane using response surface methodology, Desalin. Water Treat., 54 (2015) 966–972.
[28] C. Cojocaru, Response surface modeling and optimization of copper removal from aqua solutions using polymer assisted ultrafiltration, J. Membr. Sci., 298 (2007) 56–70.
[29] D. Jermann, W. Pronk, M. Boller, Mutual influences between natural organic matter and inorganic particles and their combined effect on ultrafiltration membrane fouling, Environ. Sci. Technol., 2008 (42) 9129–9136.
[30] L. Ao, W. Liu, L. Zhao, X. Wang, Membrane fouling in ultrafiltration of natural water after pretreatment to different extents, J. Environ. Sci., 2016 (43) 234–243.
[31] R. Pamies, The influence of mono and divalent cations on dilute and non-dilute aqueous solutions of sodium alginates, J. Carbpol, 80 (2010) 248–253.
[32] J. Stejskal and P. Kratochvil, S.P. Armes, S.F. Lascelles, A. Riede, M. Helmstedt, J. Prokes, I. Krivka, Polyaniline Dispersions. 6. Stabilization by Colloidal Silica Particles, Macromolecules, 29 (1996) 6814–6819.
[33] K. Ma, L. Cui, Y. Dong, T. Wang, C. Da, G.J. Hirasaki, S.L. Biswal, Adsorption of cationic and anionic surfactants on natural and synthetic carbonate materials, J. Colloid Interface Sci., 408 (2013) 164–172.
[34] Y.J. Kim, T. Yun, S. Lee, D. Kim, J. Kim, Accelerated testing for fouling of microfiltration membranes using model foulants, Desalination, 343 (2014) 113–119.
[35] A.W. Zularisam, A. Ahmad, M. Sakinah, A.F. Ismail, T. Matsuura, Role of natural organic matter (NOM), colloidal particles, and solution chemistry on ultrafiltration performance, Sep. Purif. Technol., 78 (2011) 189–200.
[36] Y. Li, X. Zhang, W. Zhang, J. Wang, C. Chen, Effect of powdered activated carbon on immersed hollow fiber ultrafiltration membrane fouling caused by particles and natural organic matter, Desalination, 278 (2011) 443–446.
[37] A. Abdelrasoul, H. Doan, A. Lohi, A mechanistic model for ultrafiltration membrane fouling by latex, J. Membr. Sci., 433 (2013) 88–99.
[38] K.J. Hwang, C.Y. Liao, K.L. Tung, Effect of membrane pore size on the particle fouling in membrane filtration, Desalination, 234 (2008) 16–23.